TM-1042/101/00

TECHNICAL MEMORANDUM

(TM Series)

This document was produced by SDC in performance of U. S. Government Contracts

A SAGE Long-Range-Radar Simulation Model

by

R. L. Dugas

March 15, 1963

SYSTEM DEVELOPMENT CORPORATION
2500 COLORADO AVE.
SANTA MONICA
CALIFORNIA

A SAGE LONG-RANGE-RADAR SIMULATION MODEL

by

R. L. Dugas

There have been several treatises on pulsed search radar (e.g., 4,7)* and also on SAGE-type radars (e.g., 3, 5) which utilize radar-data-processing machines. The problem of characterizing the output data is virtually impossible due to the complex factors which influence the propagation of radar pulses and their reflection from aircraft targets. Often (e.g., 2, 3, 4, 6, 7) a simplifying assumption is made which allows a mathematical treatment of the problem. In (6) Swerling treats two types of target fluctuations: non-fluctuating targets, and targets with independent Rayleigh-distributed pulse-to-pulse fluctuations. He suggest in (6) that radar data for other types of fluctuations should be studied. This suggestion is one of the objectives in developing the Long-Range-Radar (LRR) simulation model. Because of the difficulty in treating analytically radar targets with relatively slow scintillation rates, and because of the complexity of the SAGE detection logic, it was decided to develop a mathematical model using random-sampling techniques. This model would be able to generate radar data for virtually any type of target scintillation. The output of the model would be sufficiently detailed so that all properties of the data could be studied.

A computer program designed to accomplish these objectives has been written for the AN/FSQ-7 computer at Santa Monica. The model simulates data from a single target and radar as the target follows a specified flight path. The main output of the model consists of sequences of quantized video, as they would be generated by the AN/FST-2 radar-data-processing machine when

*Throughout this document, numbers in parentheses indicate items in the list of references on page 14.

the target is scanned. Quantized video is in the one state if a received radar pulse exceeds a threshold in the AN/FST-2. The sequences of quantized video are further processed by the program to determine if the target-detection threshold has been attained. If so, the computation of the reported target azimuth is carried out, and compared with the theoretically correct target azimuth in order to determine the azimuth-reporting error. The statistics of this error as a function of range or blip-scan ratio are easily determined. The reported target azimuth is determined by the beam-splitting technique used in the AN/FST-2. This involves determining the azimuths of the target's leading and trailing edges and dividing the difference by two. The difference is referred to as run length, a quantity which is transmitted with range and azimuth to the Direction Center.

The model computes run length for each detected sequence of quantized video. This data is useful in checking the properties of the model output since there is comparable empirical data on run-length variations.

The flight path is divided into range intervals of 16 n.m. each. This provides sufficient range resolution for blip scan and other functions of range. With a radial flight path and a target speed of 500 knots, about one hour's computer time will provide enough data to give reasonably high statistical confidence in the results. This time estimate assumes that both normal and MTI video data are generated for all ranges.

The model simulates cross-section fluctuations using the concept of phase-sensitive cross section, σ_p, as defined in (1). This involves specifying individual scatterers on the target and their movement. If σ_j is the

cross section of the jth scatterer on the target, then

$$\sigma_p = \left| \sum_j \sqrt{\sigma_j}\ e^{i\phi_j} \right|^2$$

where the jth phase angle, ϕ_j, depends on the position of the jth scatterer, and the radar-wave length, λ; that is

$$\phi_j = \frac{2\pi}{d_j}\lambda$$

where d_j is the distance from the jth scatterer to a reference plane perpendicular to the line of sight. Of course, it is impossible to specify accurately the cross section of all the scatterers for all aspects. The target cross section, however, can be modeled at L-band wave lengths with reasonable accuracy by considering only the predominate scatterers. These are the scatterers whose cross sections are significant fractions of the average target cross section. The modeling work is made easier by assuming that two or more scatterers in close proximity can be represented by one scatterer. This does not significantly change the fluctuation rates generated by the model. These criteria, with the aid of other techniques of (1), are used to specify the target cross-section input data. The model assumes that, although the cross section of a scatterer may change greatly over a wide aspect angle interval, it does not change during the brief exposure time when the radar beam sweeps past the target. The cross-section fluctuations during exposure time are generated by the variations in the d_j distances as a result of the target's

angular movement relative to the reference plane. The sharp rise in cross section at certain aspect angles due to the edges of wing and tail surfaces is accomplished by assuming that the target consists of only two nearly equal scatterers located at the ends of each edge.

The movement of the scatterers is generated entirely by yaw movements. This assumption is made since there is evidence that pitching, rolling, and air-frame flexing generally contribute little to cross-section fluctuations compared to yaw movements. The yaw movements are determined by two jaw rates: the yaw rate caused by the movement of the target along the flight path and a statistically varying yaw rate which takes into account variations due to air turbulence. The second yaw rate varies from scan to scan following a normal distribution. Both yaw rates remain constant during exposure time.

Target cross section, target range, and radar characteristics are combined in the radar-range equation to determine predetector signal-to-noise power ratio. The following decibel form of the radar-range equation is used:

$$SP/NP = \sigma + 2G - 4R + K$$

where σ is target cross section, G is antenna gain, and R is target range, all in db above convenient units. The antenna gain is computed from the expression

$$G = G_o \left(\frac{\sin ZW}{ZW} \right)^4$$

where G_o is the antenna gain along the beam axis, W is the angle between the beam axis and the line from radar to target, and B is a constant depending on beam width. The values of G for values of W corresponding to pulses are precomputed and become an input table for the model. The constant K accounts for all other required radar characteristics and also takes into account a unit conversion factor. K contains several constants which are difficult to specify; however, by applying the model to some situation for which a blip-scan curve has been accurately established, it is easy to accurately determine K.

Predetector signal-to-noise ratio (a) is obtained from

$$SP/NP = 10 \log_{10} \frac{a^2}{2}$$

Probability of pulse detection as obtained from (3) is

$$P(a) = \int_v^{\infty} vdv\, e^{\frac{-v^2 + a^2}{2}} I_o(av)$$

where v is the normalized amplitude threshold in the quantizer (the pulse detector) and I_o is a modified Bessel function of the first kind and zero order. A series expansion is used to calculate P(a). It is given by

$$P(a) = 1 - e^{\frac{a^2}{2}} \left\{ \sum_{n=o}^{\infty} \frac{1}{n!} \left[1 - \sum_{k=o}^{n} \frac{P_N (2.8134)^k}{k!} \right] \left(\frac{a^2}{2} \right)^n \right\}$$

where P_N is the probability that receiver noise alone will cause the pulse detector to go to the one state. Thirteen terms of the first sum insure adequate accuracy in the calculation of P(a). In SAGE radars, P_N is fixed at some level. The expression for P(a) is precomputed and tabulated as an input for the model. Singel-delay moving-target indicator (MTI) video is simulated in the model by multiplying the signal-to-noise ratio by an MTI-response factor before determining the probability of pulse detection. The response factor is a sinusoidal function of radial velocity (V_R) radar prf (F) and wave length (λ). It is zero at blind speeds and rises to a maximum of 0.9005 between blind speeds.

The expression used is

$$\frac{4}{\pi\sqrt{2}} \left| \sin\left(\frac{2\pi V_R F}{\lambda} \right) \right|$$

The model determines P(a) for every pulse of every scan during exposure time. Before and after exposure time it is assumed that $P(a) = P_N$ for enough radar pulses to insure proper detector action. Both probabilities are sampled to generate sequences of quantized video. The statistical variation in the sequences is influenced by target-aspect angle, range, scatter cross sections, scatter movement, and the horizontal antenna-gain pattern.

In its present form, the model is only two dimensional. It appears that introducing a third dimension in describing scatterer movement is unnecessary. The height effects on the radar-gain pattern have not been included, but could be taken into account in future work. The most serious omission is

the multipath effect; however, this generally occurs only when the terrain or water surrounding the radar is smooth. It seems reasonable to interpret the data as being representative of a typical situation. There is evidence from the results of an application that bears this out.

The model has been exercised for one type of radar and target. Two flight paths have been used. One is a straight radial path going from maximum to minimum range. The other path consists of two straight paths joined by a circular curve. The straight paths are chosen so that the aspect-angle variation covers a large interval.

The pulse-to-pulse cross-section fluctuations were quite different from those of either (4) or (7). Even for a relatively high yaw-rate standard deviation, the magnitude of consecutive cross sections could not be considered independent.

Distribution curves for cross-section data sampled from the pulse corresponding to the center of the beam were constructed. For the radial path, the data resembled a Poisson distribution. Using the other path, a thirty-degree change in aspect angle gave data which was more like a Rayleigh distribution. The occurrence of Rayleigh-distributed cross-section data is discussed in (9) and elsewhere. In (8) it is pointed out that L-band cross sections need not be Rayleigh distributed. On the basis of the model assumptions, and because of the lack of empirical L-band cross-section fluctuation data, it is reasonable to assume that the data generated is realistic.

Blip-scan curves were compiled for both flight paths. The data for the radial path, with a very small variation in aspect angle, agreed well with empirical blip-scan curves. The path with a large variation in aspect angle produced a blip-scan curve which diverged considerably from that of the average target. This data is shown in Figure 1. Although most empirical blip-scan curves seem to be compiled from radial-flight-path data, it is not unreasonable to find that the blip-scan function changes substantially when the flight path gives a wide variation in aspect angle. Generation of this kind of data should be more realistic than sampling fixed blip-scan curves in order to simulate SAGE data trails.

The distribution of run lengths for the radial-flight path agreed well with empirical run-length distributions for a large number of random targets with random aspect angles. For this reason it was decided to examine this data in more detail. The composition of the sequences was further analyzed by computing distribution curves for the frequency of occurrence of various "solidities." The solidity of a sequence is defined as the maximum number of consecutive hits in the sequence. Three sample spaces were used: the space consisting of all data for all ranges, and the data for the range intervals with blip-scan ratios of 35 per cent and 58 per cent. These distribution curves are shown in Figure 2. Although the beam width of the radar corresponded to 16 radar pulses, there were many sequences with solidities greater than this. It is curiously interesting to note that the distribution curves for the 35 and 58 per cent blip-scan range intervals are quite similar. Both extend from solidity 2 through 19. Both have median values which are between

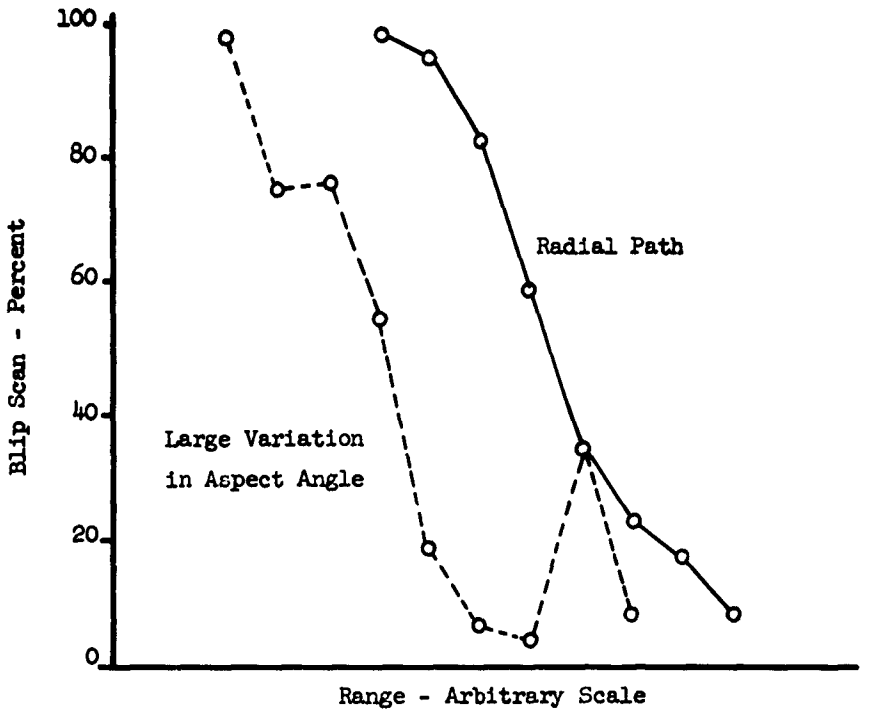

Figure 1

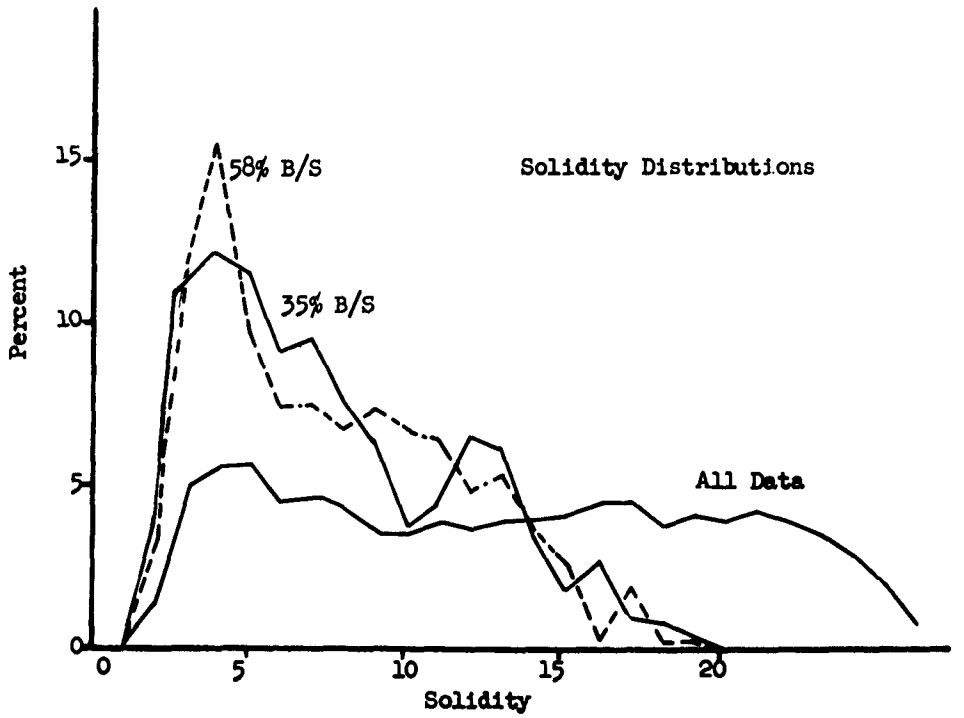

Figure 2

solidity 6 and 7, and both have the most frequent solidity of 4. The distribution curve for the space of all the data is almost uniform between solidities 3 and 23. This shows the uninitiative nature of sequences of quantized video, and the difficulty in characterizing them. To say, for example, that a sequence of a certain number of consecutive hits would be representative of a certain blip-scan ratio would not make much sense on the basis of these results. Another procedure is to say that the hits are uniformly distributed over the width of the beam. Suppose, for example, one considered the space consisting of all combinations of eight hits and eight misses. The solidity-distribution curve for this space is substantially different from any of those of Figure 2. It rises to a sharp peak of 43.1 per cent at solidity 3.

The radial-path data was further examined to determine the variation in azimuth-reporting accuracy. It was found that the mean azimuth-reporting error varied somewhat with received signal strength. This result has some influence on the best azimuth-counter preset. The best preset is discussed in (2), where this dependence is not noted. An analysis of the radial-flight-path data showed that the mean azimuth-reporting error became about one-half azimuth count larger as the blip-scan ratio varied from its highest to lowest values. This means that, because of signal-strength variations, random azimuth-reporting errors can introduce a one-azimuth-count bias, even when the best azimuth counter preset is used.

The standard deviation of azimuth-reporting errors was computed for the radial-flight path as a function of range. For comparative purposes, the model was rerun, using a target with a single scatterer with the same cross

section as the average target cross section of the previous runs, and the standard deviation of azimuth-reporting errors was computed. This gave data for a comparable nonfluctuating target. These results are shown on Figure 3 which also includes plots of the theoretical minimum standard deviation (6) for the same target and radar, assuming that the target is either not fluctuating or has independent, Rayleigh-distributed, pulse-to-pulse fluctuations. It is interesting to note that both sets of data are similar, except for extreme ranges. The difference in the levels of the two sets of data could probably be explained by quantization errors and the fact that the AN/FST-2 uses a detector logic which is not quite as good as the ideal observer theory used in (6). The difference in the shapes of the curves at extreme ranges is difficult to explain. The model data for the fluctuating target does not continue to rise at extreme ranges as does the theoretical data, but tends to converge with the nonfluctuating data. It should be pointed out that the sample size gets smaller with range; but an additional set of runs for the fluctuating target produced the same effect. More study of the model's behavior is needed to explain this effect.

From (2) a comparable estimate of the standard deviation of the azimuth-reporting error for a "weak target" has been obtained. The standard deviation is equivalent to 0.05 beam widths. This value seems to be low compared to the rest of the data of Figure 3. To the author's knowledge there is no empirical data which could be compared with Figure 3.

Scan-to-scan data for the radial path with both the fluctuating and nonfluctuating target was obtained by the model. The data was reduced to

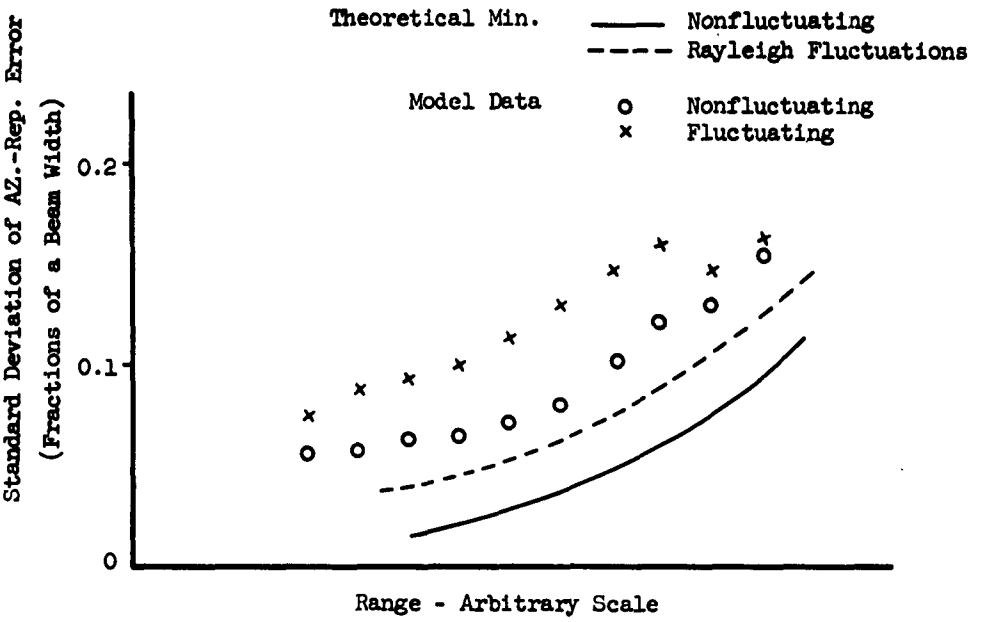

Figure 3

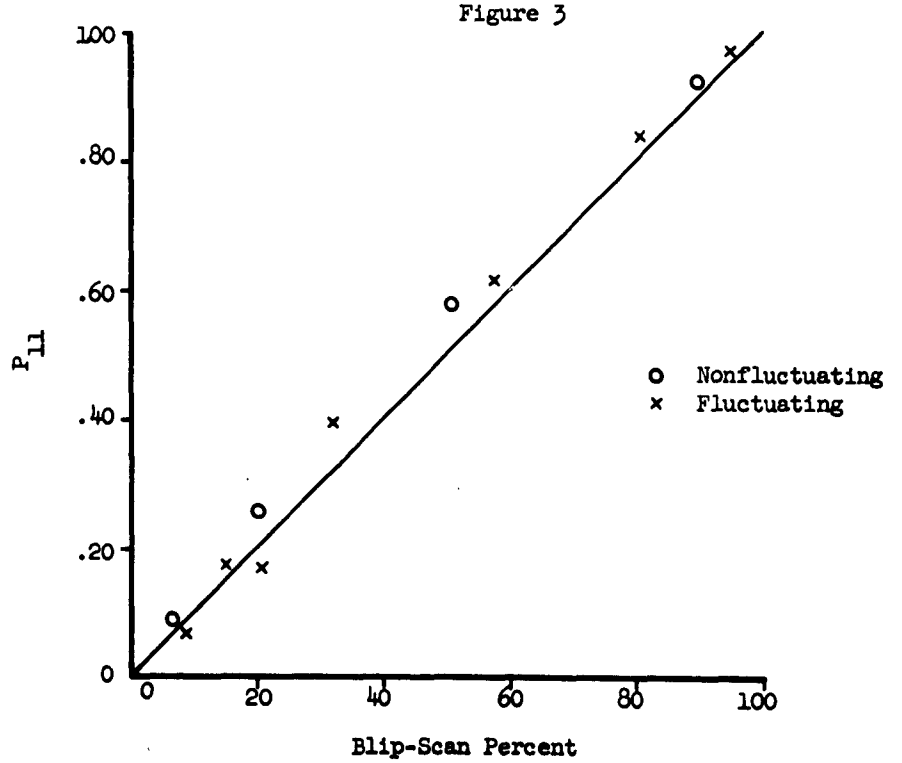

Figure 4

determine the scan-to-scan persistency of detectable sequences as the blip-scan ratio changes. It has been shown (8) that some empirical data exhibits scan-to-scan persistency which can be characterized as a second-order Markov process. The expression describing the process is:

$$P_{11} = 1 - \alpha (1 - \beta)$$

where P_{11} = probability that a detectable sequence is followed by a detectable sequence.

β = blip-scan ratio

α = a constant

Different values of α produce straight lines on Figure 4, above the diagonal and passing through $P_{11} = 1$, $\beta = 1$. Data along the diagonal ($\alpha = 1$) indicates scan-to-scan independence (i.e., $P_{11} = \beta$).

Figure 4 shows that the model data exhibits no scan-to-scan correlation in addition to that implied by β. None was to be expected for the non-fluctuating target. The fluctuating target produced variations which were high enough to be considered independent from scan to scan. It is the opinion of the author that a small yaw-rate standard deviation, when used with a flight path having a very low rate of change in aspect angle may give rise to scan-to-scan data which lies well above the diagonal of Figure 4. This and other aspects of the model's behavior remain to be studied in further applications of the model.

REFERENCES

1. Crispin, J. W., Goodrich, R. F., and Siegal, N. M. A Theoretical Method for the Calculation of the Radar Cross Sections of Aircraft and Missiles. Radiation Laboratory, Department of Electrical Engineering, College of Engineering, University of Michigan, July 1959.

2. Greenberg, L. and Pearlman, N. A Study of AN/FST-2 Azimuth Accuracy. Product Improvement Bulletin No. 9, Burroughs Corporation, March 15, 1958.

3. Harrington, J. V. An Analysis of the Detection of Repeated Signals in Noise by Binary Integration. Technical Report No. 13, Lincoln Laboratory, Massachusetts Institute of Technology, August 14, 1952.

4. Marcum, J. I. A Statistical Theory of Target Detection by Pulsed Radar. The RAND Corporation, Research Memorandum RM-754, December 1, 1947.

5. Project Lion. Beam Splitting and Search Radar Simulation. Final Report F/A-VIII, Department of Electrical Engineering, Electronics Research Laboratories, Columbia University, September 30, 1954.

6. Swerling, P. Maximum Angular Accuracy of a Pulsed Search Radar. Proceedings of the I. R. E., 44 (9), September 1956.

7. Swerling, P. Probability of Detection for Fluctuating Targets. The RAND Corporation, Research Memorandum RM-1217, March 17, 1954.

8. Symposium on Radar Detection Theory, O. N. R. Symposium Report ACR-10, Office of Naval Research, March 1-2, 1956.

UNCLASSIFIED

System Development Corporation,
Santa Monica, California
A SAGE LONG-RANGE-RADAR
SIMULATION MODEL.
Scientific rept., TM-1042/101/00,
by R. L. Dugas. 15 March 1963, 15p.,
8 refs., 4 figs.
Unclassified report

DESCRIPTORS: Programming (Computers).
Radar Range Computers

Reports that a mathematical model
using random-sampling techniques has
been developed, to simplify the UNCLASSIFIED

---

analytical treatment of radar targets UNCLASSIFIED
with relatively slow scintillation
rates. This was necessary because of
the complexity of the SAGE detection
logic. States that this model is
able to generate radar data for
virtually any type of target
scintillation. Describes a computer
program written for the AN/FSQ-7
computer at Santa Monica. UNCLASSIFIED